

Dynamical Chaos

December 7, 2008

Progress in computing lead to the discovery of apparently chaotic behavior of systems with few degrees of freedom in 70th. The systems in question can be either mechanical or nonmechanical, including examples from chemistry, biology, etc. Mathematically the models involved are described by systems of differential equations describing their dynamics, so that one calls them *dynamical systems* and the chaos found in them *dynamical chaos*.

Two different kinds of dynamical chaos are observed in *conservative* and *dissipative* systems, that is, in systems without and with relaxation.

Observation of chaos requires a sufficient time. For this reason, dynamical chaos can take place in systems with variables evolving within a finite range but there is usually no chaos in scattering problems.

The signature of dynamical chaos are apparently irregular trajectories that differ drastically from regular periodic or multiperiodic trajectories. Irregularity means that the form of trajectories is very complicated and seemingly unpredictable. The latter implies great sensitivity of trajectories to initial conditions. Although trajectories are deterministic and repeated numerical solutions yield the same result, a slightest change of initial conditions (or any parameter of the problem) leads to a completely different trajectory. Two trajectories with very close initial conditions are diverging exponentially with time. This is the mathematical criterium of the dynamical chaos. Practically, great sensitivity to initial conditions or problem parameters makes trajectories not well defined. This stimulates ideas of statistical description of such systems.

Dynamical chaos in systems with few degrees of freedom differs from the *molecular chaos* in macroscopically large systems. The latter is not necessary a real chaos but rather our way of thinking of large systems. Since it is difficult to follow the motion of an Avogadro number $N_A \sim 10^{23}$ of different particles, coarse-grained variables such as particle's density are introduced. To justify reduced description, statistical concepts such as molecular chaos are used. In fact, even regular motion of many-particle systems may be apparently chaotic. An example is the model of a harmonic oscillator coupled to a bath of harmonic oscillators that obeys linear equations of motion. Statistical properties of this model can be described with perfectly regular solutions of the dynamical equations. In general, in large systems the effect of dynamical chaos (defined in the preceding paragraph) and that of a large number of degrees of freedom coexist. It is the latter and not the former that is responsible for macroscopic behavior of large systems.

Below different aspects of the dynamical chaos will be discussed. At first we consider conservative systems and then discuss different behavior of dissipative systems.

1 Dynamical systems and degrees of freedom

The common feature of the systems showing dynamical chaos is that mathematically they are described by systems of *nonlinear* differential equations

$$\dot{x}_i = f_i(\{x_i\}, t), \quad i = 1, 2, \dots, N. \quad (1)$$

Mechanical problems can be put into the above form if one considers coordinates and velocities (or momenta) of particles as independent variables. In particular, Newtonian equations of motion for one particle with one degree of freedom can be written as

$$\begin{aligned} \dot{x} &= v \\ \dot{v} &= \frac{1}{m} F(x, v, t). \end{aligned} \quad (2)$$

Explicit time dependence in the rhs of Eq. (1) is equivalent to an additional dynamical variable t that obeys the equation

$$\dot{t} = 1. \quad (3)$$

Thus a system of N differential equations of the type of Eq. (1) with explicit time dependence is mathematically equivalent to an extended system of $N + 1$ differential equations without explicit time dependence. One can speak of the effective number of degrees of freedom as $N/2$, if the explicit time dependence is represented as an additional equation. For instance, Eq. (2) without explicit time dependence has 1 degree of freedom, whereas the same with explicit time dependence has $3/2$ degrees of freedom.

Dynamical chaos can exist in systems starting with $3/2$ degrees of freedom. For 1 degree of freedom the phase space of the system is two dimensional and trajectories cannot cross each other. (Crossing of two different trajectories would contradict the uniqueness of the solution of the dynamical problem with the initial condition set at the would be crossing point.) This imposes a severe restriction on the form of trajectories making them streamline and regular. For $3/2$ degrees of freedom, trajectories fill a three-dimensional space, so that the non-crossing condition becomes irrelevant and trajectories can meander unrestrictedly and independently from each other.

Integrals of motion restrict the solution and make dynamical chaos less likely. To count the effective number of the degrees of freedom N_F relevant to the dynamical chaos, one has to subtract the number of integrals of motion N_I from the number of equations and then divide by 2:

$$N_F = \frac{1}{2} (N - N_I). \quad (4)$$

If Eq. (2) does not have explicit time dependence and the energy is conserved, thus $N_F = 1/2$. For a motion in a central field, there are 3 degrees of freedom and thus $N = 6$ equations. However, there are also $N_I = 4$ integrals of motion, the energy and three components of the angular momentum \mathbf{L} . Thus $N_F = 1$ and there is no chaos. Adding a non-central field breaks conservation of at least one of the \mathbf{L} components and N_F increases above 1. This can lead to dynamical chaos.

2 Conservative systems

2.1 Integrable and non-integrable systems, KAM theorem

Clearly, $N_F \geq 3/2$ does not automatically imply that dynamic chaos is developing in a system. A counter-example is a *separable* system of a large numbers of uncoupled particles. Although for the whole system N_F is large, the problem splits up into many subproblems for individual particles with $N_F \leq 1$ and hence there is no chaos.

Another example is small oscillations in systems with many degrees of freedom. Approximating potentials by quadratic functions near the minima, one obtains *linear* equations of motions that can be decoupled by changing to the normal modes. Again, there is no dynamical chaos in such systems, and the example explains why dynamical chaos requires nonlinearity of the equations.

The two examples above are so-called *integrable systems* that allow separation of variables immediately or after some manipulations. There are also nonlinear dynamical systems in which separation of variables can be done and solution can be obtained in a closed form. All integrable systems do not show dynamical chaos. Each uncoupled subsystem of a large system performs a periodic motion with its own period. Thus the motion of the whole system is multiperiodic and geometrically it can be represented as regular motion on a multi-dimensional torus (circle for one degree of freedom and a simple torus for two degrees of freedom).

The simplest way to obtain an integrable nonlinear dynamical system is to start with an uncoupled dynamical system that can be easily integrated and make a transformation of variables that results in a coupled dynamical system. The latter may look complicated but it is integrable since the transformation to original variables is known.

If the starting point is a coupled nonlinear dynamical system, it is usually difficult to prove that a transformation leading to separation of variables exists. Systems that cannot be integrated by separation of variables are called *non-integrable systems* and they can show chaos. However, there is no straightforward integrability criterion. The deficiency of this definition is thus that it relies on the skills of an individual researcher.

An important question is what happens if a small perturbation is added to an integrable system so that the latter becomes non-integrable. Does it lead to dynamical chaos? Is the regular motion on a torus destroyed? The answer is given by the Kolmogorov-Arnold-Moser (KAM) theorem:

- *If*
 - *The perturbation is small*
 - *The periods of the unperturbed problem are incommensurate*

then the motion remains confined to a vicinity of the torus, except for a small subset of initial conditions

That is, all or almost all trajectories remain regular if a small non-integrable perturbation is added. The proof of this theorem is very sophisticated. Further, one can ask what are possible scenarios of the onset of dynamical chaos as the strength of the perturbation is increased. In particular, if all trajectories remain regular for a small perturbation, there should be a threshold for the chaos onset on the perturbation strength. What are trajectories just above the chaos threshold: Strongly chaotic or regular with a small chaotic component?

2.2 Divergence of trajectories and Lyapunov exponents

As stated above, the mathematical criterium of the dynamical chaos is a strong divergence of initially close trajectories with time. Usually divergence of trajectories, as instability, is described in literature by exponential dependences of the type

$$s(t) = s(0)e^{\lambda t}, \quad (5)$$

where $s(t)$ is the appropriately defined distance between two initially close trajectories. In Eq. (5) λ is the Lyapunov exponent, the same as in the theory of stability/instability. If $\text{Re } \lambda > 0$, the two trajectories exponentially diverge. Eq. (5) is idealized, however, and it is difficult to obtain λ for particular models.

To study Lyapunov exponents, one can consider two close trajectories, $x_i(t)$ and $x_i(t) + \delta x_i(t)$ and linearize Eq. (1) in $\delta x_i(t)$. This yields the system of linear differential equations for δx_i

$$\delta \dot{x}_i = \sum_{k=1}^N \frac{\partial f_i}{\partial x_k} \delta x_k, \quad i, k = 1, 2, \dots, N \quad (6)$$

with coefficients $\partial f_i / \partial x_k$ depending on time at least through $x_i(t)$. Since in the case of dynamical chaos the problem is non-integrable and thus it cannot be solved analytically for $x_i(t)$, analysis of Eq. (6) is problematic. On the top of it, even if $\partial f_i / \partial x_k$ were known, systems of linear differential equations with variable coefficients cannot usually be solved analytically. Anyway, their solution does not have a simple exponential form of Eq. (5).

A toy model for which Lyapunov exponents can be calculated is the so-called Sinai billiard. It is a two-dimensional region bounded by concave walls. Particles freely fly between the walls and elastically rebound from them like the light from a convex mirror. If two trajectories (straight in the region between the walls) make a small angle α with each other, the angle after reflection will be the same multiplied by $n > 1$ depending on the wall curvature and the angle of incidence. The number $n - 1$ plays the role of the Lyapunov exponent.

A simple practical way to test dynamical chaos is to solve Eq. (1) numerically for two close trajectories and look if they diverge. Usually the behavior of trajectories depends on where they originate. Some trajectories

do not diverge and thus are regular, other trajectories diverge and thus are chaotic. Even better is to solve Eq. (1) for one trajectory $x_i(t)$ and then to solve Eq. (6) for the linear deviation $\delta x_i(t)$. This does not require high numerical accuracy that is needed to subtract two close trajectories.

2.3 Fourier analysis

Another tool to analyze dynamical chaos is Fourier analysis of the trajectories, taking particular components $x_i(t)$. In the case of regular motion $x_i(t)$ is multiperiodic with periods T_p and each of the periodic motions is, in general, anharmonic. Thus the Fourier spectrum is discrete and consists of spikes at fundamental frequencies $\omega_p = 2\pi/T_p$ and their harmonics $\omega_{pn} = 2\pi n/T_p$. In the case of dynamical chaos the motion is not strictly periodic and there is a continuous component in the Fourier spectrum, although discrete components are present as well.

2.4 Poincaré maps

One more method to analyze regular and chaotic behavior of trajectories is the method of Poincaré maps. This method was initially proposed for conservative systems with two degrees of freedom, thus $N_F = 3/2$. Motion of such systems is confined to the three-dimensional hyperspace of constant energy within the four-dimensional phase space. Visualizing such trajectories is difficult, and the method of Poincaré maps simplifies the presentation by looking only at, say, variables x and \dot{x} for, say, $y = 0$, whereas \dot{y} is fixed by the energy conservation law and thus is not independent. Although the information in Poincaré maps is reduced, they give a very good idea of the behavior of the system. In the case of regular motion, there are usually two incommensurate periods. As a result, after a sufficiently large computation time successive points (x, \dot{x}) fill curves in the plane that is a signature of a regular motion. To the contrary, in the case of chaotic motion points (x, \dot{x}) look randomly placed. One can plot different trajectories, including regular and chaotic ones, on the same plot. The method of Poincaré maps is more sensitive to the weak chaos (predominantly regular motion with a random chaotic component) than the Fourier analysis.

A simplified version of the method of Poincaré maps is plotting points (x, \dot{x}) after equal time intervals. This version of the method does not require to solve equations of motion for $y(t) = 0$ and it is especially convenient for systems with an explicit periodic time dependence (periodically driven systems). In this case one just plots (x, \dot{x}) with the period of the external perturbation. For a system with one degree of freedom ($N_F = 3/2$) regular trajectories have a period incommensurate with that of the external perturbation, thus the points (x, \dot{x}) fill closed orbits. For more than one degree of freedom, the chosen pair of variables (x, \dot{x}) , or any other pair of variables, is multiperiodic in the case of regular motion, so that the Poincaré maps become more and more complicated. As the number of degrees of freedom increases, the Poincaré map resembles more and more that of a chaotic motion, even if the motion is regular. This is the *molecular chaos* mentioned above, as opposed to the dynamical chaos in systems with few degrees of freedom.

2.5 Example 1: Separatrix chaos in a driven double-well system

An important example of dynamical chaos in conservative systems is the separatrix chaos in a driven one-dimensional mechanical system with mass m and a double-well potential,

$$U(x, t) = \frac{kx_0^2}{8} \left[1 - \left(\frac{x}{x_0} \right)^2 \right]^2 - F(t)x, \quad F(t) = F_0 \sin(\omega t), \quad (7)$$

described by the equation of motion

$$m\ddot{x} = -\frac{\partial U(x, t)}{\partial x}. \quad (8)$$

The coefficient in Eq. (7) is chosen so that the frequency of free harmonic oscillations near the potential minima at $x = \pm x_0$ is $\omega_0 = \sqrt{k/m}$. Linearization of Eq. (8) in the deviation δx from the trajectory $x(t)$

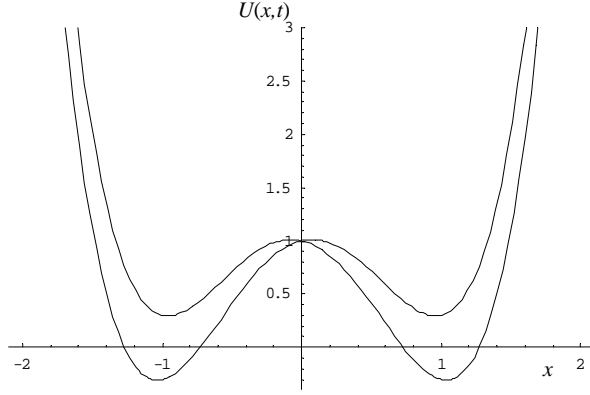


Figure 1: The double-well potential biased by the external force at different moments of time, $k_0 = 8$, $x_0 = 1$.

yields the linear equation

$$m\delta\ddot{x} = -\frac{\partial^2 U(x,t)}{\partial x^2}\delta x \quad (9)$$

that is a form of Eq. (6). Explicitly in our case one has

$$\delta\ddot{x} + \omega_0^2 \left[3 \left(\frac{x}{x_0} \right)^2 - 1 \right] \delta x = 0, \quad \omega_0^2 = \frac{k}{m}. \quad (10)$$

The concrete form of $U(x,t)$ can differ from that of Eq. (7) but an important thing is the saddle that in our example is located at $x = x_{\text{sad}} = 0$ and corresponds to the energy

$$E = E_{\text{sad}} = kx_0^2/8 \quad (11)$$

for $F = 0$. Trajectories with $E < E_{\text{sad}}$ are bounded to the left or right potential wells, whereas trajectories with $E > E_{\text{sad}}$ go over both wells. The trajectory with $E = E_{\text{sad}}$ separates both kinds of trajectories and it is called separatrix. In the presence of a time-dependent force $F(t)$ the saddle and the separatrix change with time. The instantaneous position of the saddle is defined by

$$0 = \frac{\partial U(x,t)}{\partial x} = -\frac{kx_0^2}{8} 2 \left[1 - \left(\frac{x}{x_0} \right)^2 \right] \frac{2x}{x_0^2} - F(t) \quad (12)$$

This cubic equation can be solved perturbatively for small force by setting $x \rightarrow 0$ in the square brackets. This yields

$$x_{\text{sad}}(t) \cong -\frac{2F(t)}{k}, \quad E_{\text{sad}}(t) \cong \frac{kx_0^2}{8} + \frac{F^2(t)}{k}. \quad (13)$$

This means that particles with the energy close to the saddle energy can go over the barrier between the two wells or not, depending on the instantaneous value of the force $F(t)$. Of the two close trajectories in the vicinity of the separatrix, one can go over the barrier and the other not, that means divergence of trajectories and dynamical chaos.

Indeed, numerical calculations show that for small force amplitude F_0 the trajectories in the vicinity of the separatrix become chaotic while trajectories far from the separatrix remain regular. This is in accord with the KAM theory saying that for a small non-integrable perturbation most of the trajectories remain regular and only a very small subset of trajectories become chaotic. The separatrix is exactly the chaotic

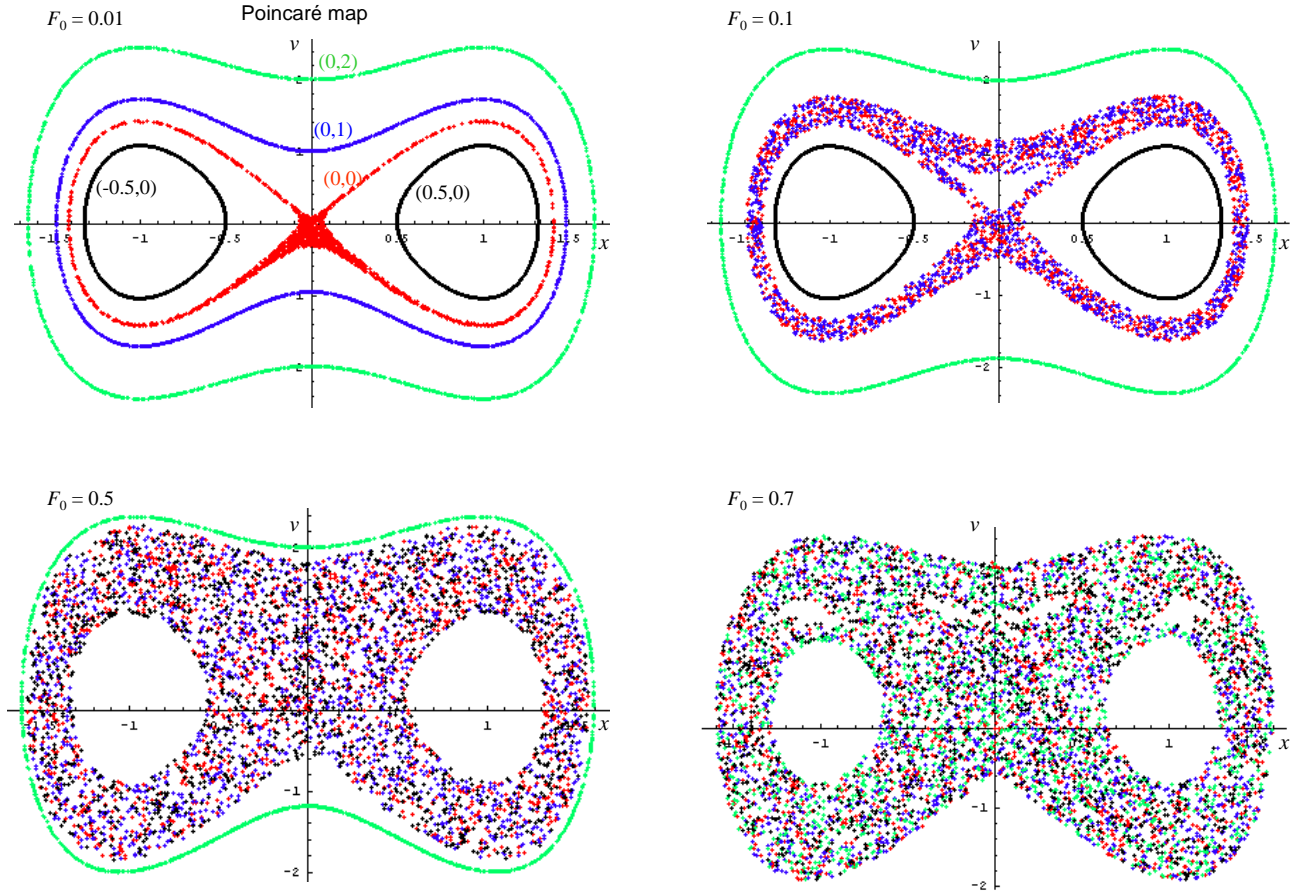


Figure 2: Poincaré maps for the driven double-well system with different amplitudes of the driving force F_0 . The trajectories are labeled in the first panel by their initial conditions $(x(0), v(0))$. With increasing F_0 more and more trajectories became chaotic, starting from the separatrix, and the phase volume of the chaos increases.

trajectory referred to in the KAM theorem. With increasing F_0 the region of chaos around the separatrix becomes broader.

The results of numerical solution with $m = 1$, $k = 8$, $x_0 = 1$, and $\omega = 1$ are presented in Fig. 2 for different amplitudes of the force F_0 and different initial conditions $(x(0), v(0))$. First, Poincaré maps taken with the period of the external force $2\pi/\omega$ show chaotization of trajectories with increasing F_0 , starting from the trajectories near the separatrix. When the separate regular trajectories merge into chaos, they become the same chaotic trajectory, no matter what were the initial conditions. For $F_0 = 0.7$ (the last panel) all trajectories shown are chaotic. Since the Poincaré maps contain a lot of points, the chaotic region is well defined by its boundaries. The regions with no points in the last panel correspond to the regions of regular motion. With increasing F_0 up to 2 the regular regions near the two potential minima disappear in chaos.

Let us now investigate the divergence of trajectories. We at first solve Eq. (8) with some initial conditions and then Eq. (9) with the initial condition $\delta x(0) = \delta v(0) = \delta$ with $\delta = 10^{-50}$. The distance between the trajectories (the divergence) is defined as

$$s(t) \equiv \sqrt{[\delta x(t)]^2 + [\delta v(t)]^2}. \quad (14)$$

Other initial conditions for δx and δv and other definitions of s would serve well, too. In Fig. 3 one can see that near the separatrix (left panel, red) there is a strong divergence of trajectories (i.e., the dynamical chaos)

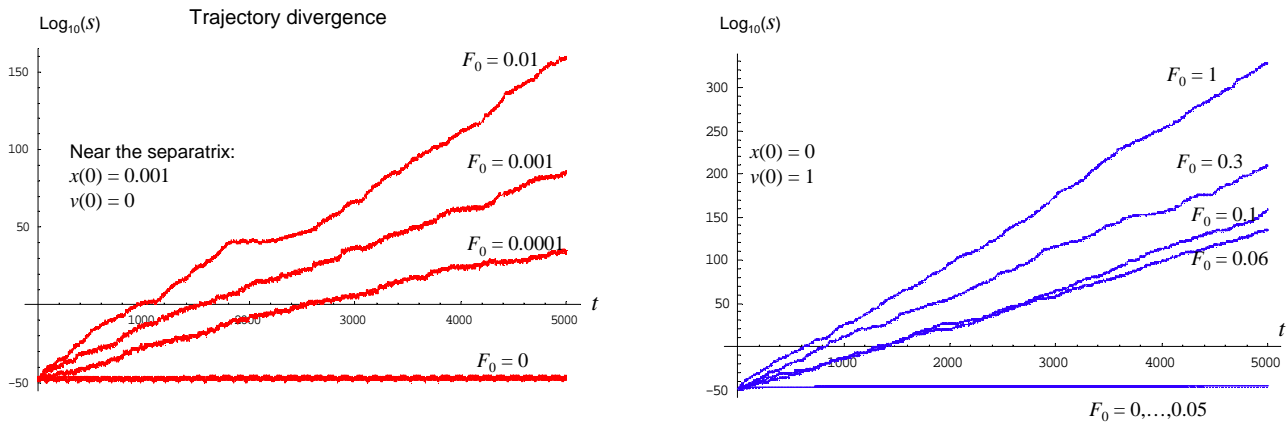


Figure 3: Divergence of trajectories. Left panel: Near the separatrix trajectories become chaotic already for very small F_0 . Right panel: Away from the separatrix trajectories become chaotic only for sufficiently strong perturbation, according to the KAM theorem. The colors match those in the Poincaré maps above.

even for very small F_0 . For trajectories away from the separatrix (right panel, blue) chaos is a threshold phenomenon. In the particular case shown, it occurs for $F_0 \gtrsim 0.05$. Note that the exponential law of Eq. (5) is obeyed only on average, as argued above. The large deviations $|\delta x| \gg 1$ seen in Fig. 3 are, of course, unphysical, as linearization of equations requires small $\delta x(t)$. In reality, $|\delta x|$ defined as the distance between two trajectories, will saturate at $|\delta x| \sim 1$. Still, this form of presentation gives a good idea of the chaos, and the formal problem with large δx can be solved by taking δ appropriately small.

2.6 Example 2: Chaos in a strongly driven one-well system

Another example of the dynamical chaos in driven systems with one degree of freedom is described by the model with the quartic potential

$$U(x, t) = \frac{kx_0^2}{4} \left(\frac{x}{x_0} \right)^4 - F(t)x, \quad F(t) = F_0 \sin(\omega t). \quad (15)$$

There is no separatrix in this model, thus there is no reason for any particular trajectory to become chaotic already for a very small F_0 . This model is a pure example of the KAM theorem with the dynamical chaos emerging above a threshold on F_0 , so that below the threshold all trajectories remain regular. The Poincaré maps calculated with $m = 1$, $k = 4$, and $\omega = 1$ are shown in Fig. 4. The threshold of chaos in this case is comparable to that for the trajectories away from the separatrix in the double-well model. Note that one can see different separated from each other chaotic trajectories in the Poincaré maps.

One can ask why the Poincaré maps, especially the last panel in Fig. 4, are nonsymmetric with respect to the transformation $v \rightarrow -v$, although the problem is symmetric. The answer is that the Poincaré maps is only a tool to visualize chaos but they do not provide a full description of trajectories since only a small subset of points is used. The Poincaré points in Fig. 4 are taken with the period of $F(t)$ at $t = 0, T, 2T$, etc. At these times $F(t) = 0$ but $\dot{F}(t) > 0$ that breaks the symmetry of the problem with respect to velocities. Choosing another periodic set of Poincaré points that is shifted by a constant amount results in a different Poincaré map that is not symmetric with respect to both x and v , in general. Thus the exact form of the Poincaré map is not very significant.

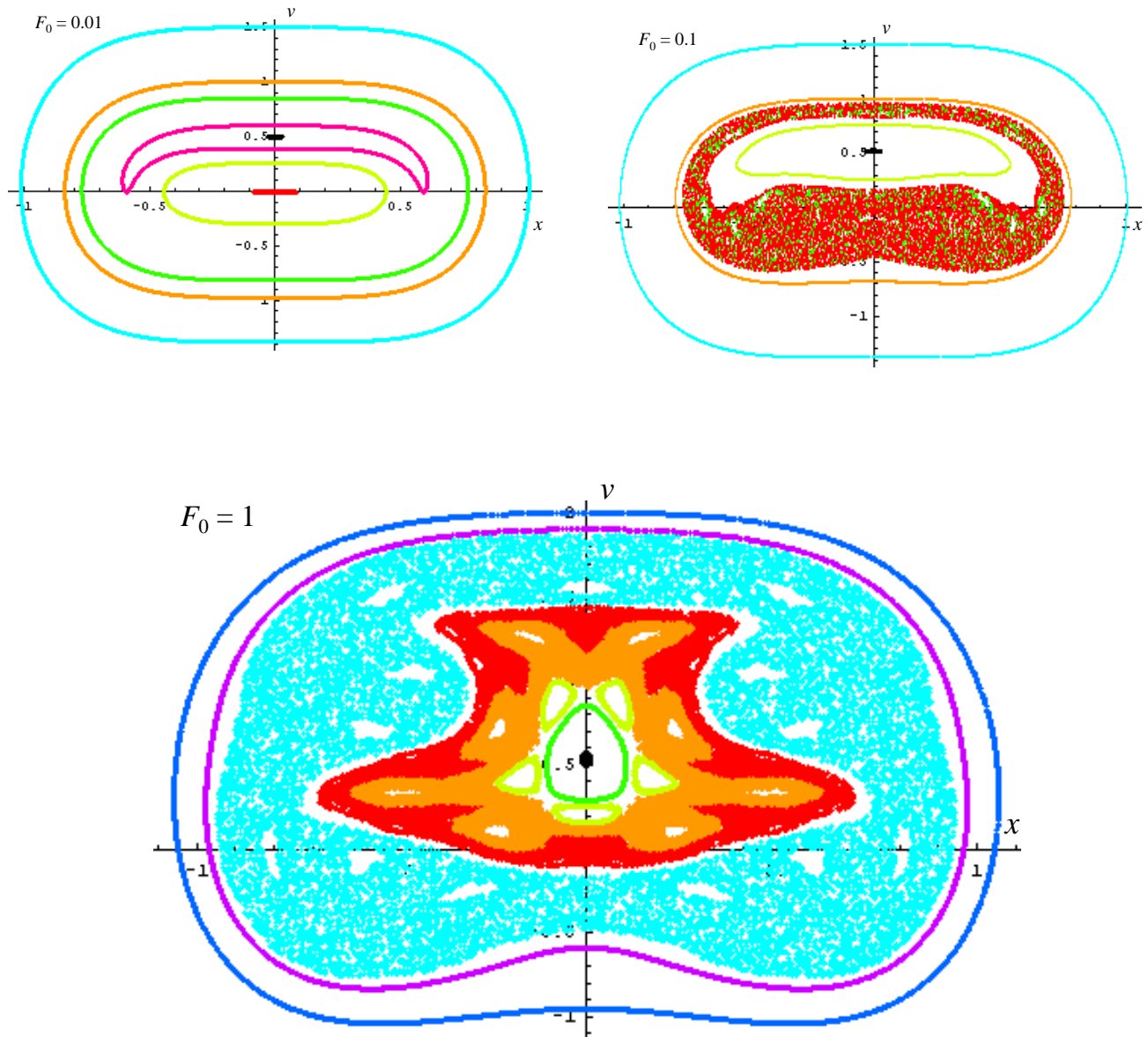


Figure 4: Poincaré maps for the driven system with a quartic potential with different amplitudes of the driving force F_0 . In this model dynamical chaos emerges above a threshold on F_0 . Below the threshold all trajectories remain regular. With increasing F_0 above the threshold more and more trajectories become chaotic.

3 Dissipative systems

In the presence of dissipation, a mechanical system relaxes down to one of its local energy minima. Trajectories in the phase space are asymptotically approaching the points $(x = x_{\min}, v = 0)$ that are called *point attractors*. Point attractors have dimension zero. In non-physical systems such as chemical and biological systems, there may be point attractors, too, that do not correspond to any energy minimum. A more complicated system is a generator that asymptotically approaches a stationary time-dependent state being a cycle in the phase space. This state is called a limiting cycle or a *cycle attractor*. A more simple example of a cycle attractor is the stationary motion of a dissipative system (such as a damped oscillator) under the influence of a periodic force. In the simplest case, the system follows the force, so that the period of the cycle attractor coincides with that of the force. This is the *simple cycle attractor*. In the case of one degree of freedom, the cycle attractor is a line and its dimension is one. The Poincaré map corresponding to a simple cycle attractor, taken with the period of the external force, consists of a single point.

Generally, dissipation tends to make chaotic motion regular. For instance, in the case of a driven double-well system trajectory beginning in the chaotic region near the separatrix will leave this region with time and approach a simple cycle attractor, that is a regular motion. Chaos in dissipative systems is a threshold phenomenon on the amplitude of the driving force F_0 , friction constant γ , or other parameters. The onset of chaos in dissipative systems manifests itself in the system response going out of synch with the applied periodic force. This happens via a sequence of *bifurcations* that change the system's behavior discontinuously. A typical first bifurcation is a period doubling after which the system does not return completely to its initial state after one period of the force, the mismatch being small close to the bifurcation threshold. However, after two periods of the external force the system returns to its initial state. Further increase of the control parameter leads to the increase of the mismatch after one external period, followed by another bifurcation. This can be another period doubling or, in general, period multiplying. This makes the motion of the system more complicated, the attractor becoming a *multiple cycle attractor*. The number of external periods in the multiple cycle attractor is the number of points on the Poincaré map. The dimension of this kind of attractors is still the same as that of the corresponding simple cycle attractor. The Fourier spectrum is discrete and consists of the fundamental frequency corresponding to the period of motion of the system and its harmonics.

After a few bifurcations the motion of the system can become *incommensurate* with the external force. This increases the dimension of the attractor. For instance, in the case of one degree of freedom the simple and multiple cycle attractors are closed contours and they have dimension one. An incommensurate cycle attractor is a torus and it has dimension two. The Poincaré map corresponding to this kind of attractor consists of many points that fill a line after a sufficient amount of data is generated.

With further increase of the control parameter chaos breaks in as the final bifurcation. The chaotic state of a driven dissipative system is also a kind of attractor that is reached after some transient time. The structure of chaotic attractors is complicated. Looking at the Poincaré map it is difficult to judge about the exact dimension of the attractor. It seems to be between two and three for one degree of freedom since the points on the Poincaré map fill two-dimensional regions but not in a dense way. Magnification of regions in the Poincaré map (that costs a lot of computation time to generate enough data) shows a self-similar, i.e. *fractal*, structure. The same patterns infinitely repeat themselves upon magnification. One can extend the definition of dimensionality upon fractals and it turns out to be non-integer, indeed. As the motion on a chaotic attractor is non-periodic, the Fourier spectrum is continuous. Still there are spikes as discrete frequencies, the same as for the regular motion.

Lyapunov exponents for the motion on attractors can be obtained by linearizing the equation of motion in the deviation δx as above. Of course, this should be done skipping the transient time needed to approach the attractor. For regular attractors, the Lyapunov exponents are negative, that is, the initially created trajectory deviation disappears with time because of dissipation. For chaotic attractors, on the contrary, the Lyapunov exponents are positive, so that initially close trajectories diverge without leaving the attractor. It should be stressed that Eq. (5) that defines Lyapunov exponents is obeyed only on average since chaotic

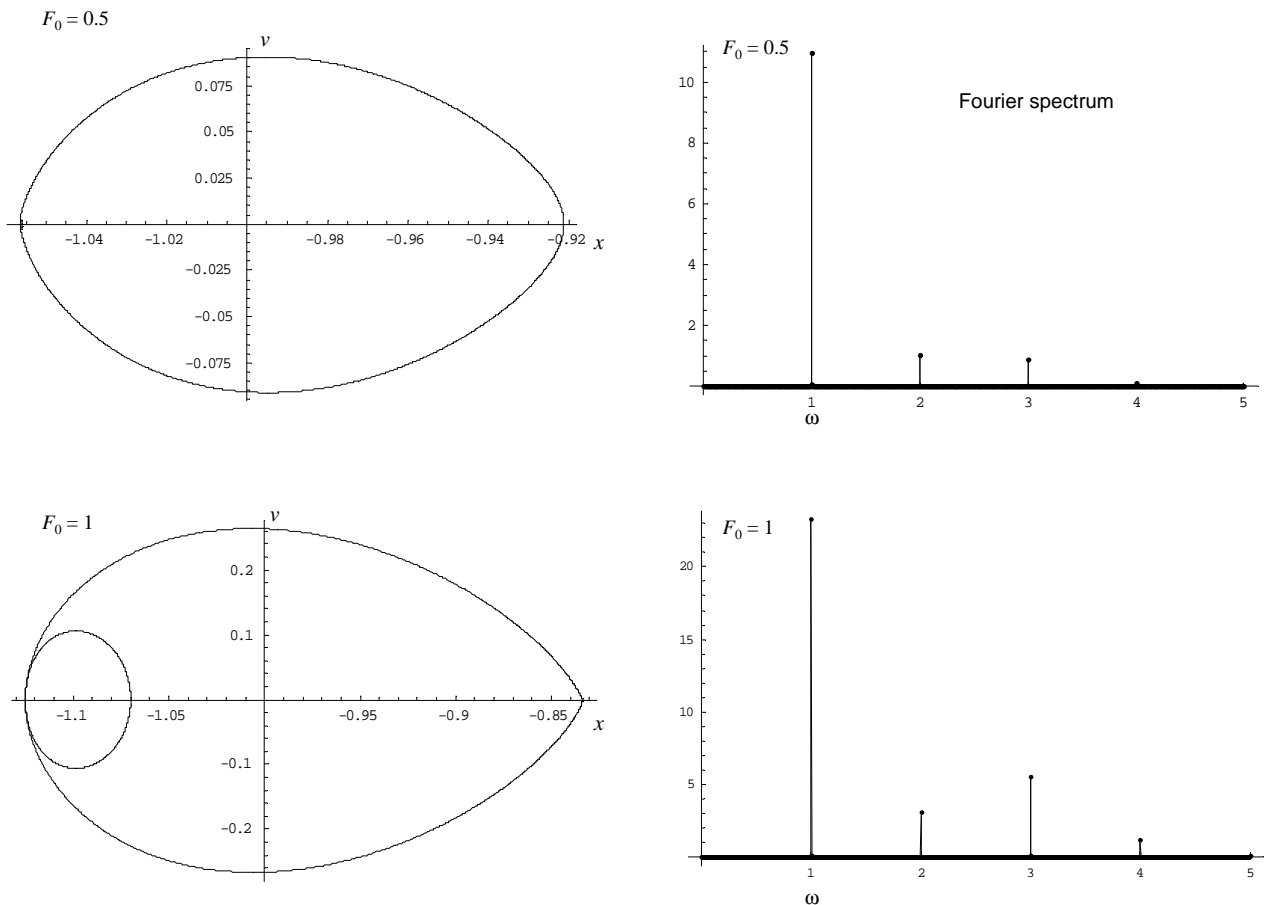


Figure 5: Attractors and Fourier spectra for the driven dissipative double-well model with small sinusoidal force, $F_0 = 0.5$ and 1 . In both cases the attractor is located in one well. Intensity of harmonics of the fundamental frequency ω increase with F_0 .

solutions cannot have an exact simple exponential form.

3.1 Example: Driven double-well system with dissipation

As an example consider the driven double-well system described by Eq. (7) with added damping γ , so that the equation of motion has the form

$$m\ddot{x} + \gamma m\dot{x} = -\frac{\partial U(x,t)}{\partial x}. \quad (16)$$

First, fix $m = 1$, $k = 8$, $\omega = 1$, and $\gamma = 0.01$ and study the attractor for different values of the force amplitude F_0 . For $F_0 < F_{0c} = (2/\sqrt{3})^3 \simeq 1.54$ the potential $U(x,t)$ has two minima at all times. Thus there should be two simple cycle attractors around each of the minima. The system ends up in one of them depending on the initial condition. This behavior is seen in Fig. 5.

For larger force amplitudes such as $F_0 = 1.5$ and 2 in Fig. 6, attractors extend over both wells. Note that only one of the two possible attractors is shown for $F_0 = 1.5$. Another attractor can be obtained by the reflection $x \rightarrow -x$. For $F_0 = 2$, to the contrary, the attractor is symmetric and unique. More important, it is a triple cycle attractor. One can see the peak at the frequency $\omega/3$ in the Fourier spectrum. The period-tripling bifurcation occurs between $F_0 = 1.9$ and $F_0 = 1.95$. There is no period doubling for the chosen values of parameters in this model. Further, around $F_0 = 2.05$ the inverse bifurcation occurs and

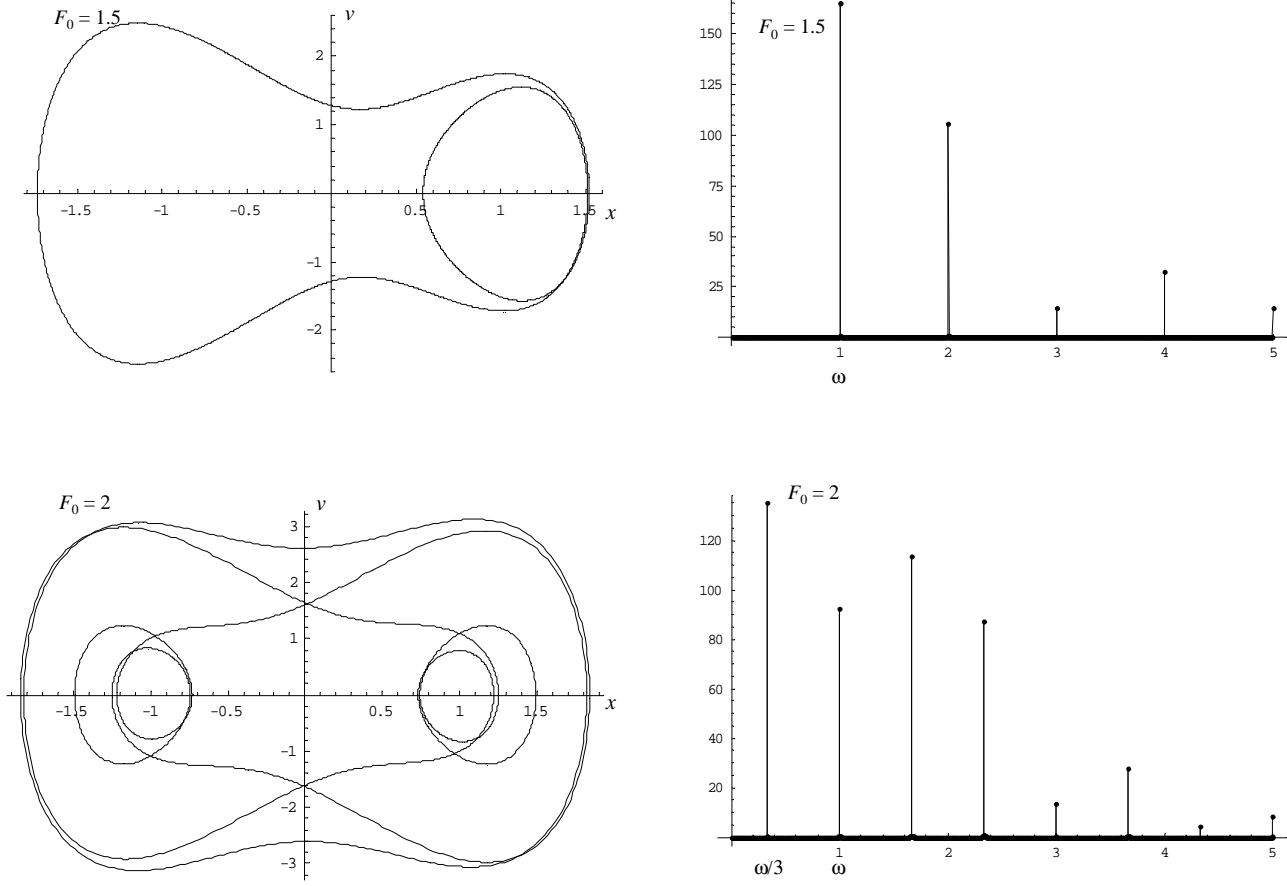


Figure 6: Attractors and Fourier spectra for the driven dissipative double-well model with larger sinusoidal force, $F_0 = 1.5$ and 2. In both cases the attractor extends over both wells.

the system returns to a simple cycle attractor. At $F_0 = 2.05$ both asymmetric simple cycle attractors and the symmetric triple-cycle attractor are realized for different initial conditions.

At $F_0 = 3.0$ (not shown) there are two asymmetric simple cycle attractors similar to $F_0 = 2$. At $F_0 = 3.3$ one obtains either one of the simple asymmetric attractors as for $F_0 = 3.0$ or a five-fold cycle attractor, depending on initial conditions. The five-fold cycle attractor is shown in Fig. 7. At $F_0 = 3.5$ the attractor is chaotic. The Poincaré maps in both cases are shown in Fig. 8. With further increase of F_0 the chaos disappears again. In particular, for $F_0 = 4.5$ there are two asymmetric eight-fold cycle attractors, for $F_0 = 5$ there are two asymmetric simple attractors, for $F_0 = 10$ there are two asymmetric double cycle attractors. In all cases, attractors with an odd number of cycles are symmetric and attractors with even number of cycles occur in asymmetric pairs.

Let us now consider the case of slow external force, $\omega = 0.1$. The force amplitude will be kept constant, $F_0 = 1.6 > F_{0c}$, so that the particle slides out of a disappearing metastable energy minimum into the stable one, approaches the stable energy minimum and tends to stay there until this minimum becomes metastable and eventually disappears, etc. The control parameter will be the damping γ . For large γ the attractor is a simple cycle, whereas for small γ it is chaotic. The attractor and its Fourier spectrum for $\gamma = 1$ are shown in Fig. 9. Decrease of γ leads to a period-doubling bifurcation, see Fig. 10 for $\gamma = 0.3$ and 0.25. For $\gamma = 0.24$ (see Fig. 11) there is already a multi-cycle attractor with about 14 cycles, as one can see on the Poincaré map. For $\gamma = 0.23$ (see Fig. 12) there is an incommensurate cycle attractor of dimension 2, since the points on the Poincaré map fill a line. Further decrease of γ lead to the increasing the length of the line in the

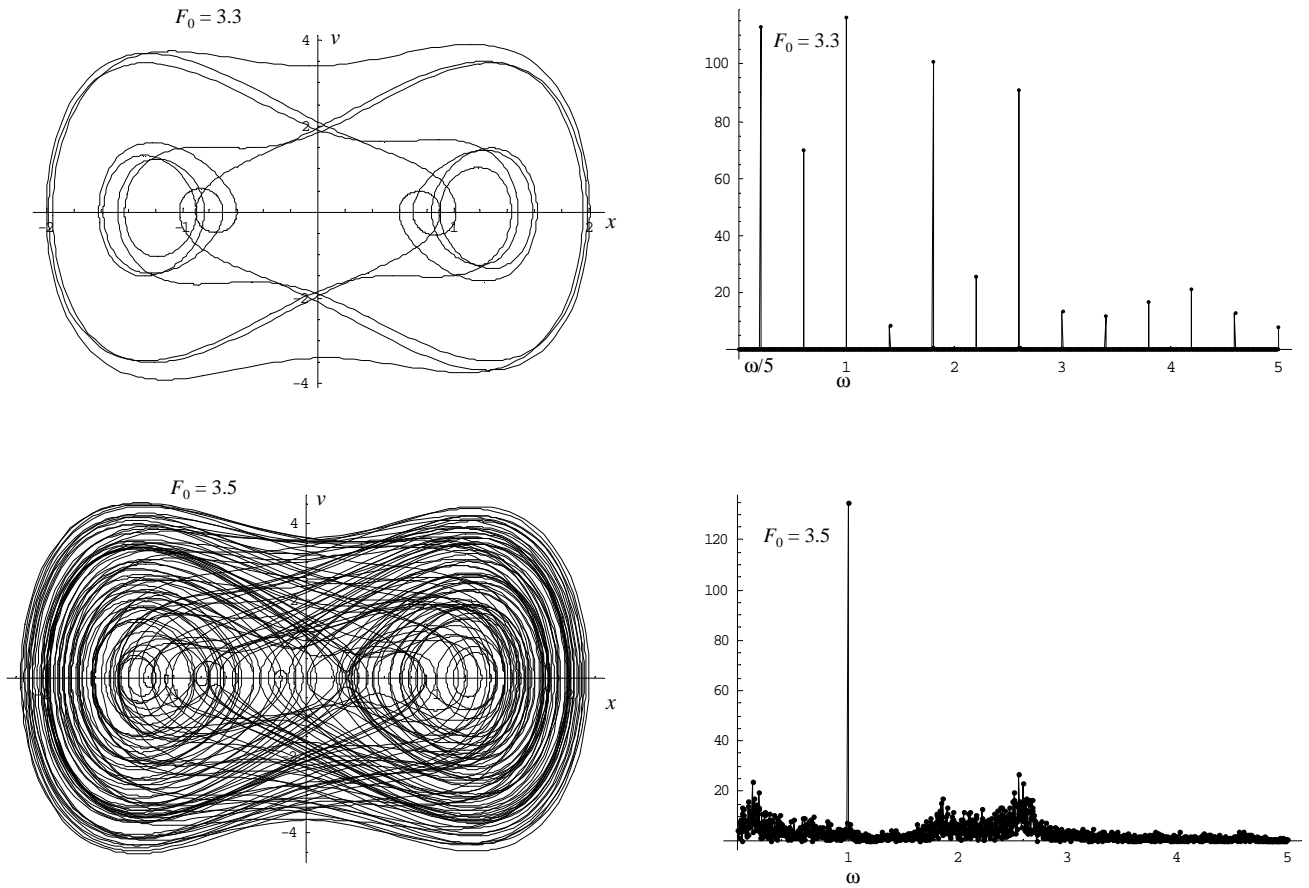


Figure 7: Attractors and Fourier spectra for the driven dissipative double-well model with $F_0 = 3.3$ (five-fold cycle attractor) and 3.5 (chaotic attractor). The Fourier spectrum for chaotic attractor is continuous with a spike at the fundamental frequency ω .

Poincaré map, that is, the size of the incommensurate attractor, see Fig. 13. For even smaller γ the form of the Poincaré map changes and the motion becomes apparently chaotic., see Fig. 14 for $\gamma = 0.03$. With further decrease of γ the chaotic attractor grows and its Poincaré map approaches that of the conservative model considered above, see Fig. 15 for $\gamma = 0.003$.

Finally, the time dependence of the trajectory deviations $s(t)$ for $\omega = 0.1$, $F_0 = 1.6$, and different values of γ are shown in Fig. 16. One can see that the borderline between the regular and chaotic behavior is $\gamma = 0.24$ where attractor becomes incommensurate with the periodic force.

Summarizing, one can say that there are a lot of different types and scenarios of dynamical chaos, so that the latter is a big zoo.

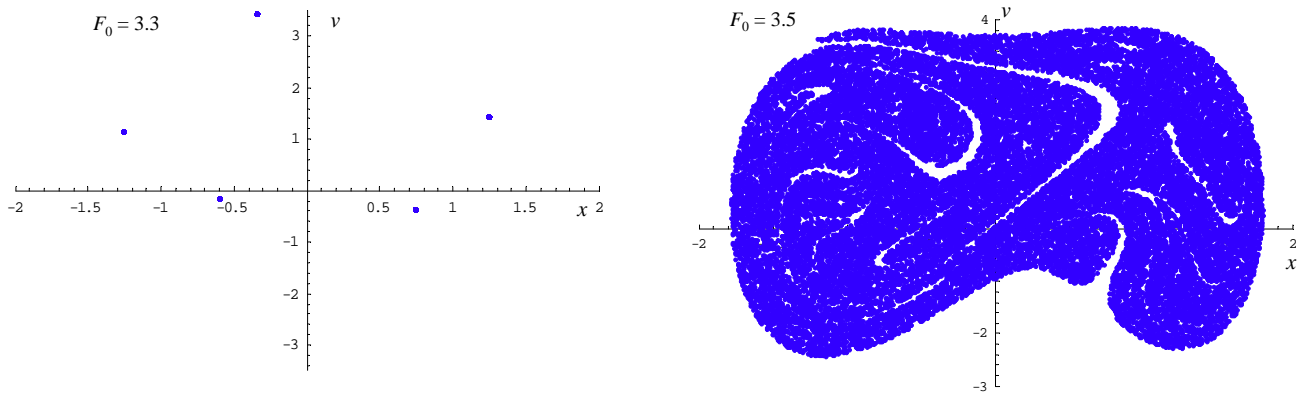


Figure 8: Poincaré maps for $F_0 = 3.3$ (five-fold cycle attractor) and 3.5 (chaotic attractor).

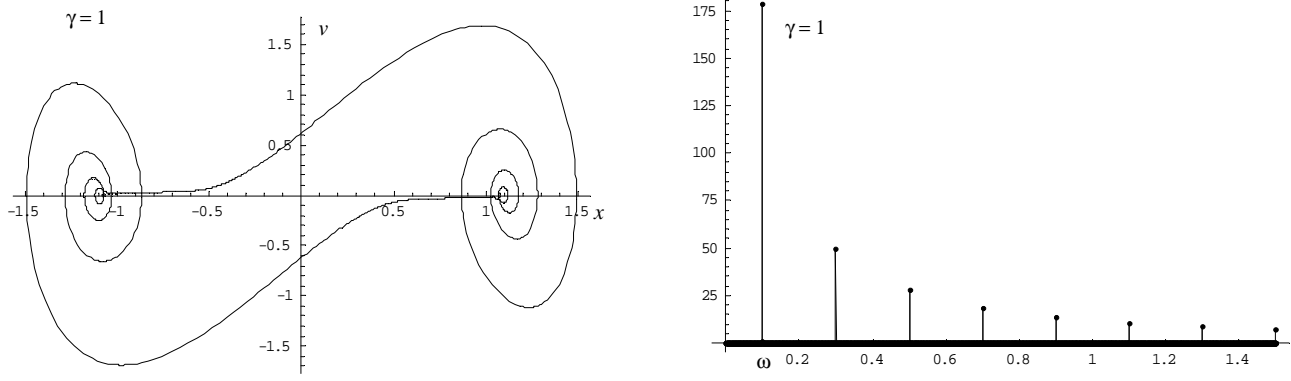


Figure 9: Simple attractor and its Fourier spectrum for $\omega = 0.1$, $F_0 = 1.6$, and $\gamma = 1$.

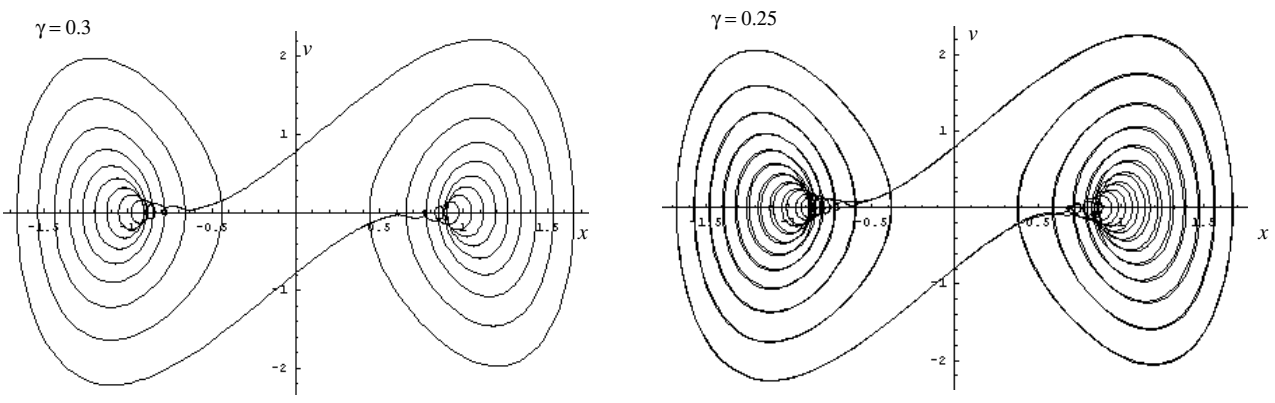


Figure 10: Simple and double-cycle attractors for $\gamma = 0.3$ and 0.25 , respectively.

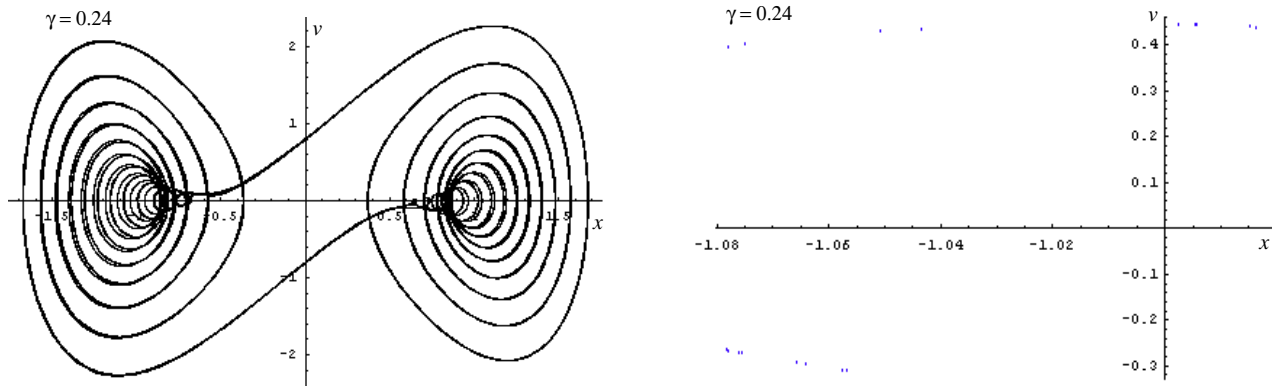


Figure 11: Multi-cycle attractor with about 14 cycles for $\gamma = 0.24$ and its Poincaré map.

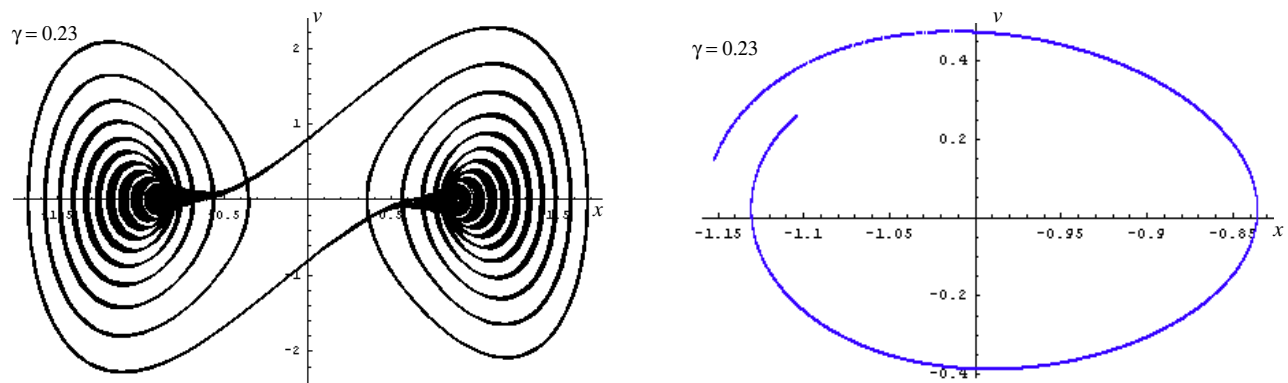


Figure 12: Incommensurate cycle attractor for $\gamma = 0.23$.

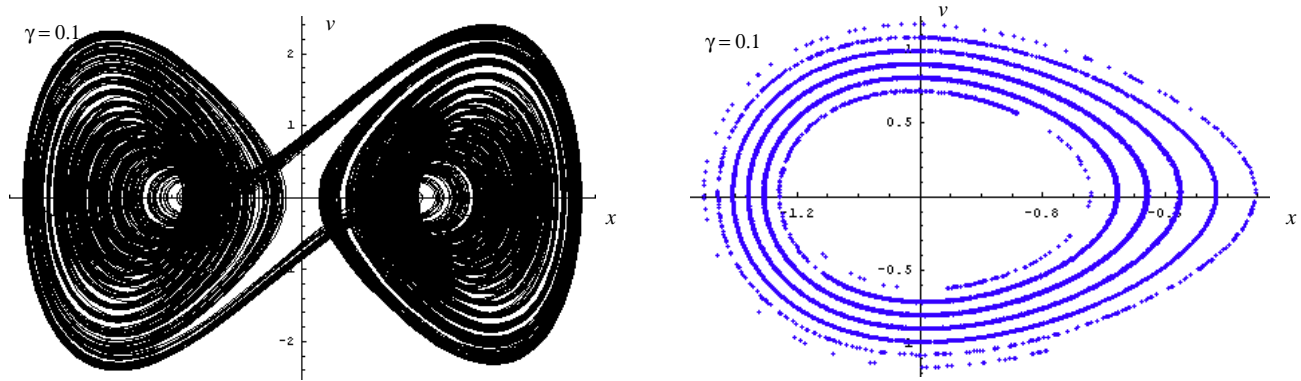


Figure 13: Incommensurate cycle attractor for $\gamma = 0.1$.

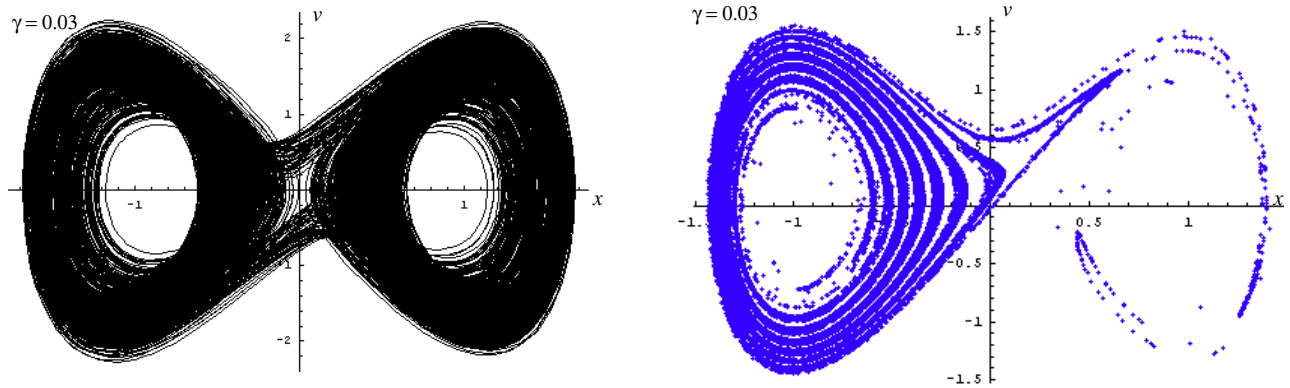


Figure 14: Chaotic attractor for $\gamma = 0.03$.

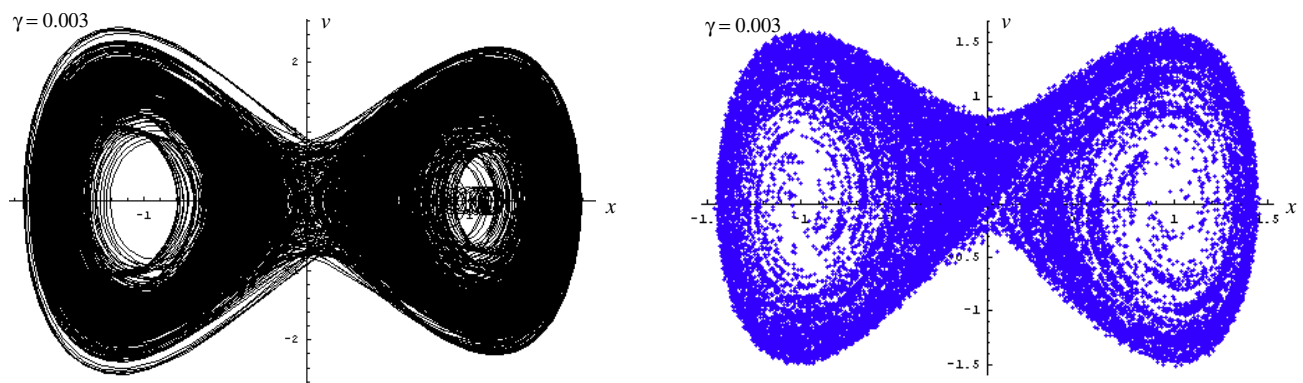


Figure 15: Attractor with a developed chaos for $\gamma = 0.003$, close to the dynamical chaos in conservative systems.

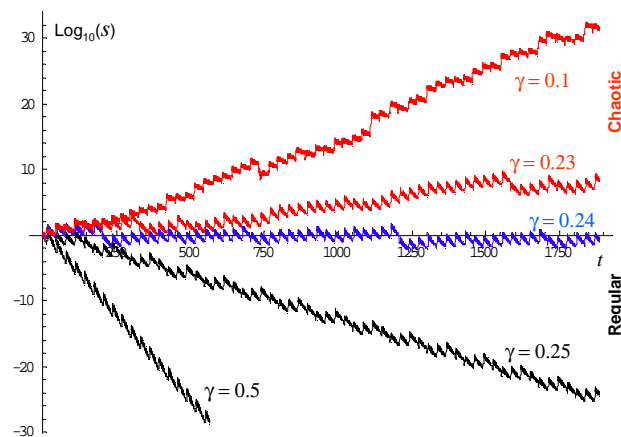


Figure 16: Trajectory deviations on the attractor for $\omega = 0.1$, $F_0 = 1.6$, and different values of γ . The borderline between the regular and chaotic behavior is $\gamma = 0.24$ where attractor becomes incommensurate with the periodic force.